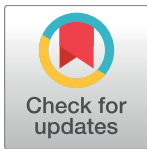


RESEARCH ARTICLE

Genome-wide association studies and CRISPR/Cas9-mediated gene editing identify regulatory variants influencing eyebrow thickness in humans

Sijie Wu¹, Manfei Zhang^{1,2,3}, Xinzhou Yang^{4,5}, Fuduan Peng⁶, Juan Zhang⁷, Jingze Tan², Yajun Yang^{2,7}, Lina Wang¹, Yanan Hu¹, Qianqian Peng¹, Jinxi Li¹, Yu Liu¹, Yaqun Guan⁸, Chen Chen⁹, Merel A. Hamer¹⁰, Tamar Nijsten¹⁰, Changqing Zeng⁶, Kaustubh Adhikari¹¹, Carla Gallo¹², Giovanni Poletti¹², Lavinia Schuler-Faccini¹³, Maria-Cátira Bortolini¹³, Samuel Canizales-Quinteros¹⁴, Francisco Rothhammer¹⁵, Gabriel Bedoya¹⁶, Rolando González-José¹⁷, Hui Li², Jean Krutmann¹⁸, Fan Liu^{6,19}, Manfred Kayser¹⁹, Andres Ruiz-Linares^{2,11}, Kun Tang^{1,2}, Shuhua Xu^{1,2,20,21}, Liang Zhang^{4,5*}, Li Jin^{1,2,3*}, Sijia Wang^{1,2,3,21*}



OPEN ACCESS

Citation: Wu S, Zhang M, Yang X, Peng F, Zhang J, Tan J, et al. (2018) Genome-wide association studies and CRISPR/Cas9-mediated gene editing identify regulatory variants influencing eyebrow thickness in humans. *PLoS Genet* 14(9): e1007640. <https://doi.org/10.1371/journal.pgen.1007640>

Editor: Gregory M. Cooper, HudsonAlpha Institute for Biotechnology, UNITED STATES

Received: May 7, 2018

Accepted: August 16, 2018

Published: September 24, 2018

Copyright: © 2018 Wu et al. This is an open access article distributed under the terms of the [Creative Commons Attribution License](https://creativecommons.org/licenses/by/4.0/), which permits unrestricted use, distribution, and reproduction in any medium, provided the original author and source are credited.

Data Availability Statement: Summary statistics for all analyzed variants for the Taizhou Han Chinese, Xinjiang Uyghur, and CANDELA GWAS datasets can be found in the National Omics Data Encyclopedia (NODE) (<http://www.biosino.org/node/>), using accession ID: OEZ000393. Individual genotype and phenotype data cannot be shared due to IRB restrictions on privacy concerns. All other relevant data are within the paper and its Supporting Information files.

1 CAS Key Laboratory of Computational Biology, CAS-MPG Partner Institute for Computational Biology, Shanghai Institute of Nutrition and Health, Shanghai Institutes for Biological Sciences, University of Chinese Academy of Sciences, Chinese Academy of Sciences, Shanghai, China, **2** State Key Laboratory of Genetic Engineering and Ministry of Education Key Laboratory of Contemporary Anthropology, Collaborative Innovation Center for Genetics and Development, School of Life Sciences, Fudan University, Shanghai, China, **3** Human Phenome Institute, Fudan University, 825 Zhangheng Road, Shanghai, China, **4** CAS Key Laboratory of Tissue Microenvironment and Tumor, Shanghai Institute of Nutrition and Health, Shanghai Institutes for Biological Sciences, University of Chinese Academy of Sciences, Chinese Academy of Sciences, Shanghai, China, **5** SIBS (Institute of Health Sciences) Changzheng Hospital Joint Center for Translational Research, Institutes for Translational Research (CAS-SMMU), Shanghai, China, **6** Key laboratory of Genomic and Precision Medicine, Beijing Institute of Genomics, Chinese Academy of Sciences, Beijing, China, **7** Fudan-Taizhou Institute of Health Sciences, Taizhou, Jiangsu, China, **8** Department of Biochemistry, Preclinical Medicine College, Xinjiang Medical University, Urumqi, China, **9** Department of Stomatology, Chang Zheng Hospital, Second Military Medical University, Shanghai, China, **10** Department of Dermatology, Erasmus MC University Medical Center Rotterdam, CA Rotterdam, The Netherlands, **11** Department of Genetics, Evolution and Environment, and UCL Genetics Institute, University College London, London, United Kingdom, **12** Laboratorios de Investigación y Desarrollo, Facultad de Ciencias y Filosofía, Universidad Peruana Cayetano Heredia, Lima, Peru, **13** Departamento de Genética, Universidade Federal do Rio Grande do Sul, Porto Alegre Brasil, **14** Unidad de Genómica de Poblaciones Aplicada a la Salud, Facultad de Química, UNAM-Instituto Nacional de Medicina Genómica, México City, México, **15** Instituto de Alta Investigación, Universidad de Tarapacá, Arica, Chile, **16** Laboratorio de Genética Molecular (GENMOL), Universidad de Antioquia, Medellín, Colombia, **17** Instituto Patagónico de Ciencias Sociales y Humanas, Centro Nacional Patagónico, CONICET, Puerto Madryn, Argentina, **18** IUF-Leibniz Research Institute for Environmental Medicine, Dusseldorf, Germany, **19** Department of Genetic Identification, Erasmus MC University Medical Center Rotterdam, CA Rotterdam, The Netherlands, **20** School of Life Science and Technology, ShanghaiTech University, Shanghai, China, **21** Center for Excellence in Animal Evolution and Genetics, Chinese Academy of Sciences, Kunming China

☞ These authors contributed equally to this work.

* zhangliang01@sibs.ac.cn (LZ); lijin@fudan.edu.cn (LJ); wangsijia@picb.ac.cn (SW)

Abstract

Hair plays an important role in primates and is clearly subject to adaptive selection. While humans have lost most facial hair, eyebrows are a notable exception. Eyebrow thickness is heritable and widely believed to be subject to sexual selection. Nevertheless, few genomic studies have explored its genetic basis. Here, we performed a genome-wide scan for

Funding: This work was supported by the "Strategic Priority Research Program" of the Chinese Academy of Sciences (grant number XDB13041000 to SW), a key basic research grant from the Science and Technology Commission of Shanghai Municipality (grant number 16JC1400504 to SW), the National Natural Science Foundation of China (NSFC) (grant numbers 91631307 to SW, 30890034 and 31271338 to LJ, 31471385 and 81673104 to LZ, 91731303, 31771388, 31525014 and 31711530221 to SX), the National Thousand Young Talents Award to SW and LZ, and a Max Planck-CAS Paul Gerson Unna Independent Research Group Leadership Award to SW, the National Basic Research Program (2015FY111700 to LJ), Shanghai Municipal Science and Technology Major Project (2017SHZDX01 to LJ), the Ministry of Education (311016 to LJ), the Chinese Academy of Sciences (No. XDB13040100 to SX), the Program of Shanghai Academic Research Leader (16XD1404700 to SX), the National Key Research and Development Program (2016YFC0906403 to SX), the National Key R&D Program of China (2017YFA0103500 and 2017YFA0102800 to LZ, Shanghai Science and Technology Development Funds 15140904200 to LZ, the National Program for Top-notch Young Innovative Talents of The "Wanren Jihua" Project to SX. Project supported by Shanghai Municipal Science and Technology Major Project (Grant No. 2017SHZDX01). The CANDELA work was funded by grants from the Leverhulme Trust (F/07 134/DF to ARL), BBSRC (BB/I021213/1 to ARL) and Institute Strategic Programme grant to The Roslin Institute), Universidad de Antioquia (GENMOL sostenibilidad 2015-2016 and MASO 2013-2014). FL is supported by the Erasmus University Rotterdam (EUR) fellowship and the Chinese "1000-Talents Program" for young scholars. The RS work was also funded by a Vidi Grant of the Netherlands Organization for the Health Research and Development (ZonMw) (no. 91711315) to TN. The generation and management of GWAS genotype data for the Rotterdam Study (RS I, RS II, RS III) was executed by the Human Genotyping Facility of the Genetic Laboratory of the Department of Internal Medicine, Erasmus MC, Rotterdam, The Netherlands. The GWAS datasets are supported by the Netherlands Organization of Scientific Research NWO Investments (nr. 175.010.2005.011, 911-03-012), the Genetic Laboratory of the Department of Internal Medicine, Erasmus MC, the Research Institute for Diseases in the Elderly (014-93-015; RIDE2), the Netherlands Genomics Initiative (NGI)/Netherlands Organization of Scientific Research (NWO) Netherlands Consortium for Healthy Aging

eyebrow thickness in 2961 Han Chinese. We identified two new loci of genome-wide significance, at 3q26.33 near *SOX2* (rs1345417: $P = 6.51 \times 10^{-10}$) and at 5q13.2 near *FOXD1* (rs12651896: $P = 1.73 \times 10^{-8}$). We further replicated our findings in the Uyghurs, a population from China characterized by East Asian-European admixture ($N = 721$), the CANDELA cohort from five Latin American countries ($N = 2301$), and the Rotterdam Study cohort of Dutch Europeans ($N = 4411$). A meta-analysis combining the full GWAS results from the three cohorts of full or partial Asian descent (Han Chinese, Uyghur and Latin Americans, $N = 5983$) highlighted a third signal of genome-wide significance at 2q12.3 (rs1866188: $P = 5.81 \times 10^{-11}$) near *EDAR*. We performed fine-mapping and prioritized four variants for further experimental verification. CRISPR/Cas9-mediated gene editing provided evidence that rs1345417 and rs12651896 affect the transcriptional activity of the nearby *SOX2* and *FOXD1* genes, which are both involved in hair development. Finally, suitable statistical analyses revealed that none of the associated variants showed clear signals of selection in any of the populations tested. Contrary to popular speculation, we found no evidence that eyebrow thickness is subject to strong selective pressure.

Author summary

Hair plays an important role in primates and is clearly subject to adaptive selection. While humans have lost most facial hair, eyebrows are a notable exception. Eyebrow thickness is heritable and widely believed to be subject to sexual selection. Nevertheless, few genomic studies have explored its genetic basis. Here we performed genome-wide association studies for eyebrow thickness in multiple ethnic groups, including Han Chinese, Uyghurs, Latin Americans, and Caucasians. We found solid evidence that novel genetic variants near the *SOX2*, *FOXD1* and *EDAR* genes could affect eyebrow thickness. After fine mapping, we prioritized four variants for experimental verification. CRISPR/Cas9-mediated gene editing provided evidence that the variants rs1345417 and rs12651896 affect the transcriptional activity of the nearby *SOX2* and *FOXD1* genes. This represents a successful example of a combination of GWAS and CRISPR/Cas9 technology to demonstrate how non-coding variants with regulatory functions may play an important role in common diseases and traits. Finally, suitable statistical analyses suggest that, contrary to popular speculation, eyebrow thickness should not be subject to strong selection pressure, including sexual selection.

Introduction

Hair has a range of important functions in primates and has been speculated to be subject to intense natural and sexual selection [1]. Although humans have lost most terminal body hair to allow the development of more efficient sweating as an adaptation to bipedal life, considerable facial hair remains, with great diversity between populations [2]. The eyebrow, an area of thick, short facial hair above the eye that follows the shape of the lower margin of the brow ridge, is one of the most conspicuous features of the face. It is thought that its main function is to prevent sweat, water, and other debris from getting into the eye [2]. As a major facial feature, the eyebrow plays an important role in human communication, facial expression, sexual dimorphism and attractiveness [3–6]. It has been suggested that eyebrows may be subject to

(NCHA), project nr. 050-060-810. The Rotterdam Study is funded by Erasmus Medical Center and Erasmus University, Rotterdam, Netherlands Organization for the Health Research and Development (ZonMw), the Research Institute for Diseases in the Elderly (RIDE), the Ministry of Education, Culture and Science, the Ministry for Health, Welfare and Sports, the European Commission (DG XII), and the Municipality of Rotterdam. The National Key R&D Program of China (2017YFA0103500 and 2017YFA0102800 to LZ, Shanghai Science and Technology Development Funds 15140904200 to LZ, the National Program for Top-notch Young Innovative Talents of The “Wanren Jihua” Project to SX. Project supported by Shanghai Municipal Science and Technology Major Project (Grant No. 2017SHZDZX01). The CANDELA work was funded by grants from the Leverhulme Trust (F/07 134/DF to ARL), BBSRC (BB/1021213/1 to ARL) and Institute Strategic Programme grant to The Roslin Institute), Universidad de Antioquia (GENMOL sostenibilidad 2015-2016 and MASO 2013-2014). FL is supported by the Erasmus University Rotterdam (EUR) fellowship and the Chinese “1000-Talents Program” for young scholars. The RS work was also funded by a Vidi Grant of the Netherlands Organization for the Health Research and Development (ZonMw) (no. 91711315) to TN. The generation and management of GWAS genotype data for the Rotterdam Study (RS I, RS II, RS III) was executed by the Human Genotyping Facility of the Genetic Laboratory of the Department of Internal Medicine, Erasmus MC, Rotterdam, The Netherlands. The GWAS datasets are supported by the Netherlands Organization of Scientific Research NWO Investments (nr. 175.010.2005.011, 911-03-012), the Genetic Laboratory of the Department of Internal Medicine, Erasmus MC, the Research Institute for Diseases in the Elderly (014-93-015; RIDE2), the Netherlands Genomics Initiative (NGI)/Netherlands Organization for Scientific Research (NWO) Netherlands Consortium for Healthy Aging (NCHA), project nr. 050-060-810. The Rotterdam Study is funded by Erasmus Medical Center and Erasmus University, Rotterdam, Netherlands Organization for the Health Research and Development (ZonMw), the Research Institute for Diseases in the Elderly (RIDE), the Ministry of Education, Culture and Science, the Ministry for Health, Welfare and Sports, the European Commission (DG XII), and the Municipality of Rotterdam. The funders had no role in study design, data collection and analysis, decision to publish, or preparation of the manuscript.

sexual selection [7]. Notably, eyebrow thickness varies between and within human populations [8,9]. A recent genome-wide association study in Latin Americans found that common DNA variants in the *FOXL2* gene are associated with eyebrow thickness. However, these variants have very low minor allele frequencies in East Asians and Europeans, suggesting that in these two populations, eyebrow thickness may well be affected by different genes.

To enhance our understanding of the genetic basis underlying the variation of human eyebrow thickness, we conducted a genome-wide association study in East Asians and Eurasians, followed by a trans-ethnic meta-analysis, to identify genetic variants that affect eyebrow thickness in humans. Moreover, in order to validate the findings from our association analyses, we performed fine mapping and conducted functional genetic experiments. Finally, we applied various statistical genetics methods to search for signals of positive selection in and around the identified candidate genes.

Results

Genome-wide association analysis identified three novel loci associated with eyebrow thickness

Our discovery GWAS included a total of 2961 subjects from the Taizhou Longitudinal Study [10] (TZL, Han Chinese). Replication cohorts were drawn from the Xinjiang Uyghur Study [11] (UYG, N = 721, Uyghur, an admixed East Asian-European population), the CANDELA study [8] (CANDELA, N = 2301, Latin Americans) and the Rotterdam Study [12,13] (RS, N = 4411, Northwestern Europeans; for sample characteristics see S1 Table). In all cohorts, eyebrow thickness was assessed on an ordered categorical scale using a self-developed photo numeric approach (S1 Fig). Inter-rater (for the CANDELA cohort, intra-rater) reliability was reasonable for all cohorts (Kappa: 0.48–0.66, S2 Table). There was a higher degree of diversity in eyebrow thickness in Uyghurs (D = 0.58, Gini-index) and Northern Europeans (D = 0.57) than in Han Chinese (D = 0.52) and Latin Americans (D = 0.49) (S1 Table). Eyebrows were significantly less thick in females than in males in TZL, UYG, and RS ($P_{TZL} = 7.23 \times 10^{-70}$, $P_{UYG} = 7.31 \times 10^{-33}$, $P_{RS} = 4.10 \times 10^{-106}$; the CANDELA sample included only male subjects). Age was negatively correlated with eyebrow thickness in TZL, CANDELA, and RS ($P_{TZL} = 7.75 \times 10^{-20}$, $P_{CANDELA} = 4.20 \times 10^{-17}$, $P_{RS} = 1.33 \times 10^{-10}$; the UYG sample included only young subjects between 18 and 24 years). The GWAS in Han Chinese was based on 7,119,456 SNPs; it identified association signals of genome-wide significance ($P < 5 \times 10^{-8}$) for two genomic regions, located at 3q26.33 (rs1345417: $P = 6.51 \times 10^{-10}$) and 5q13.2 (rs12651896: $P = 1.73 \times 10^{-8}$; Fig 1). After conditioning on the genotypes of rs1345417 and rs12651896, no additional SNPs showed significant association at a genome-wide level ($P < 5 \times 10^{-8}$). The heritability of eyebrow thickness in TZL was 37.6%. The SNPs rs1345417 and rs12651896 explain 3.11% and 2.55% of this heritability, respectively. Although the GWAS in the Uyghurs, which was based on 7,224,952 SNPs, did not detect any genome-wide significant signals (S2 Fig), the signals at 3q26.33 and 5q13.2 showed marginal significance (rs1345417: $P = 3.78 \times 10^{-4}$; rs12651896: $P = 5.4 \times 10^{-2}$), and allelic effects were consistent with those in TZL (Table 1).

The GWAS in Latin Americans has been published previously; it found that common variants at 3q22.3 are associated with eyebrow thickness [8]. We found that it also corroborated our findings at 3q26.33 and 5q13.2 (rs1345417: $P = 1.04 \times 10^{-7}$; rs12651896: $P = 7.54 \times 10^{-6}$). The meta-analysis of all three GWAS (TZL, UYG and CANDELA) identified four loci reaching genome-wide significance ($P < 5 \times 10^{-8}$; Fig 2A; S3 Table). Apart from the loci described above 3q26.33 (rs1345417: $P = 1.11 \times 10^{-19}$), 5q13.2 (rs12651896: $P = 2.52 \times 10^{-13}$) and 3q22.3 (rs112458845: $P = 2.24 \times 10^{-9}$) there was one additional locus of genome-wide significance, at 2q12.3 (rs1866188: $P = 5.81 \times 10^{-11}$) (Fig 2). The respective quantile-quantile (Q-Q) plots

Competing interests: The authors have declared that no competing interests exist.

showed no sign of inflation for any of the association tests described above, and the genomic control factor λ was relatively low in all cases ($\lambda_{\text{TZL}} = 1.041$, $\lambda_{\text{UYG}} = 1.053$, $\lambda_{\text{CANDELA}} = 1.015$, $\lambda_{\text{Meta}} = 1.040$, S3 Fig), indicating that the test statistics were not substantially confounded by population sub-stratification.

For all three novel loci (3q26.33, 5q13.2 and 2q12.3), the allelic effects acted in the same direction in all populations (Table 1). There was no significant effect size heterogeneity across populations for any of these three association signals (S3 Table). However, the signal at 3q22.3, which was highly significant in CANDELA, with $P = 4.95 \times 10^{-11}$ at rs112458845 and an effect allele frequency (EAF) of 0.127, did not reach nominal significance in our GWAS of TZL (EAF = 0.065, $P = 0.729$) and UYG (EAF = 0.032, $P = 0.494$). Furthermore, our meta-analysis revealed strong allelic heterogeneity for rs112458845 ($Q = 16.284$, $I^2 = 81.58\%$; S3 Table), indicating that the effect at 3q22.3 may be specific to Latin Americans.

We performed a further replication analysis for all SNPs described above in the Rotterdam Study sample, which comprises 4411 Dutch Europeans. With the exception of rs112458845 at 3q22.3, which was specific to Latin Americans, this analysis replicated all signals at a nominal significance level (rs1866188: $P = 0.0141$; rs112458845: $P = 0.366$; rs1345417: $P = 4.03 \times 10^{-3}$; rs12651896: $P = 2.93 \times 10^{-4}$; Table 1). The allelic effects at all associated SNPs acted in the same direction as in all other populations tested (Table 1).

Fine mapping of associated loci suggests four causal variants affecting eyebrow thickness

Next, we sought to localize the variants driving the association signals at each of the novel loci that attained genome-wide significance in our trans-ethnic meta-analysis. We utilized PAIN-TOR [14,15] to calculate the Bayesian posterior causal probability for each variant included in the signal and identified the sets of variants that collectively explained 99% of the total probability (credible sets). The credible sets for 2q12.3 and 3q26.33 contained a single SNP each (S4 Table). The credible set for 5q13.2 comprised nine variants. Among these, the posterior causal probability was highest for rs12651896 (posterior probability = 0.744; S4 Table). Using CADD [16] and DeepSEA [17] to assess the functional consequences of each variant, we found that rs10061469 was consistently predicted to be functionally important (S4 Table). Our interrogation of ENCODE [18] and REMC [19] data revealed that the regions around rs1866188 and rs1345417 show distinct active enhancer signatures defined by epigenetic markers, such as the histone modifications H3K4me1 and H3K27ac, and DNase hypersensitivity in epithelial cells (Fig 3). The regions around rs12651896 and rs10061469 are involved in long-range chromatin looping interactions with *FOXD1* (Fig 3B). Together, these data suggest the presence of putative regulatory regions in the neighborhood of these variants. We thus chose rs1345417, rs12651896, rs10061469 and rs1866188 for further experimental verification.

Validating regulatory activity within regions underlying the association signals

To further examine whether the four variants identified in our fine mapping analyses (rs1345417, rs12651896, rs10061469 and rs1866188) play a role in the expression of nearby genes, we conducted CRISPR/Cas9-mediated gene editing for each of them. We targeted the genomic regions surrounding each variant using two different sgRNAs (S4 Fig). Our qRT-PCR analysis of annotated transcripts near these SNPs found that mixed clones of A375 cells that were stably infected with rs1345417 targeting lenti-Cas9-sgRNAs displayed significantly reduced *SOX2* expression and significantly elevated *SOX2-OT* expression compared to cells infected with control lenti-Cas9-sgRNAs (Fig 4A). Infection with rs12651896 targeting lenti-

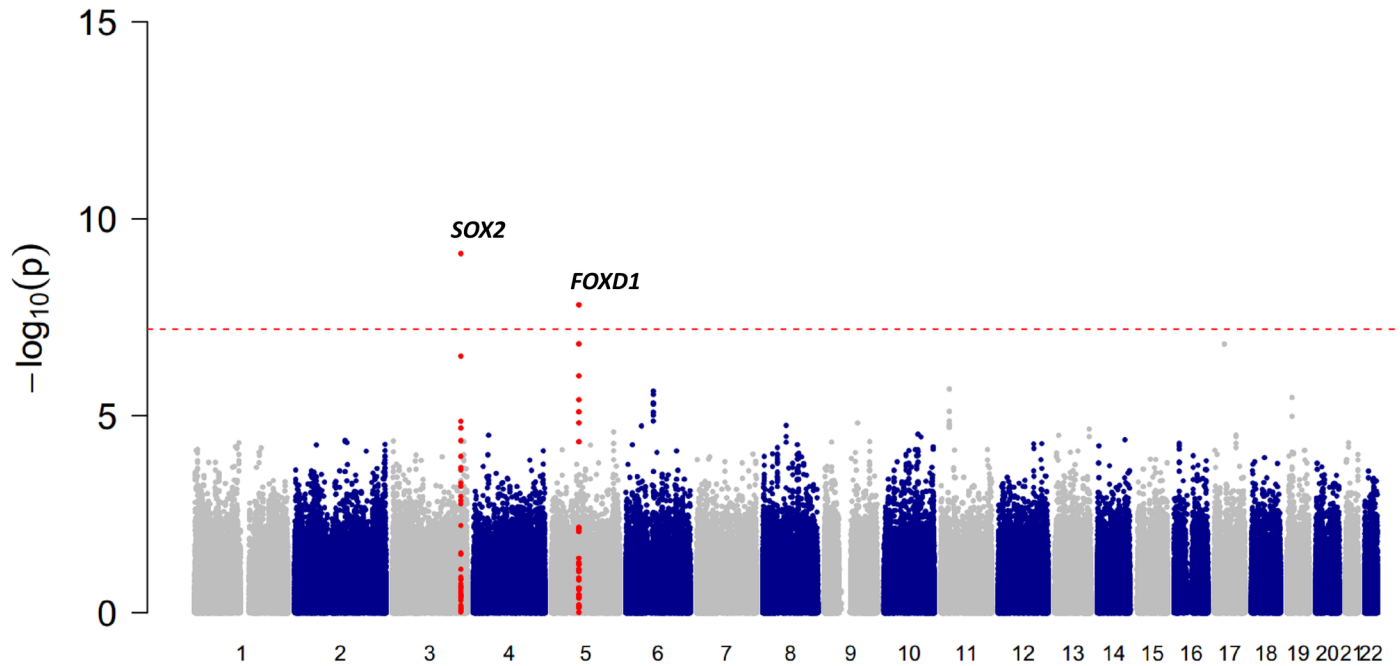


Fig 1. Manhattan plot showing the results of the GWAS for eyebrow thickness in Han Chinese. Manhattan plot illustrating the results of the genome-wide scan for eyebrow thickness in 2961 Han Chinese after adjusting for the top four PCs, gender and age. The red line indicates the threshold for genome-wide statistical significance ($P < 5 \times 10^{-8}$). Red dots represent SNPs that are close (<5 kb) to the genome-wide significant signals.

<https://doi.org/10.1371/journal.pgen.1007640.g001>

Cas9-sgRNAs led to a significant reduction in the expression of *FOXD1* (Fig 4B), while infection with rs10061469 targeting lenti-Cas9-sgRNAs showed no effect on nearby genes (Fig 4C). Infection with rs1866188 targeting lenti-Cas9-sgRNAs resulted in a significant reduction in *LIMS1* expression of (Fig 4D).

Table 1. GWAS results for lead SNPs significantly associated with eyebrow thickness.

SNP	Chr.	Position ^a	Gene	Allele	Population	Freq.	Beta	P value
rs1866188	2	109257152	EDAR (253kb up)	A	TZL	0.92	0.096	1.46×10^{-4}
					UYG	0.35	0.09	3.42×10^{-3}
					CANDELA	0.39	0.087	3.54×10^{-6}
					RS	0.06	0.064	0.0141
rs112458845	3	138675741	FOXL2	G	TZL	0.065	-0.009	0.729
					UYG	0.032	0.056	0.494
					CANDELA	0.27	-0.127	4.95×10^{-11}
					RS	0.00	0.089	0.366
rs1345417	3	181511951	SOX2 (79kb down)	G	TZL	0.27	0.092	6.51×10^{-10}
					UYG	0.54	0.105	3.78×10^{-4}
					CANDELA	0.52	0.098	1.04×10^{-7}
					RS	0.58	0.04	4.03×10^{-3}
rs12651896	5	72502029	FOXD1 (242kb down)	C	TZL	0.27	0.084	1.73×10^{-8}
					UYG	0.26	0.064	0.054
					CANDELA	0.32	0.08	7.54×10^{-6}
					RS	0.71	0.05	2.93×10^{-4}

^aPosition according to human reference NCBI37/hg19.

<https://doi.org/10.1371/journal.pgen.1007640.t001>

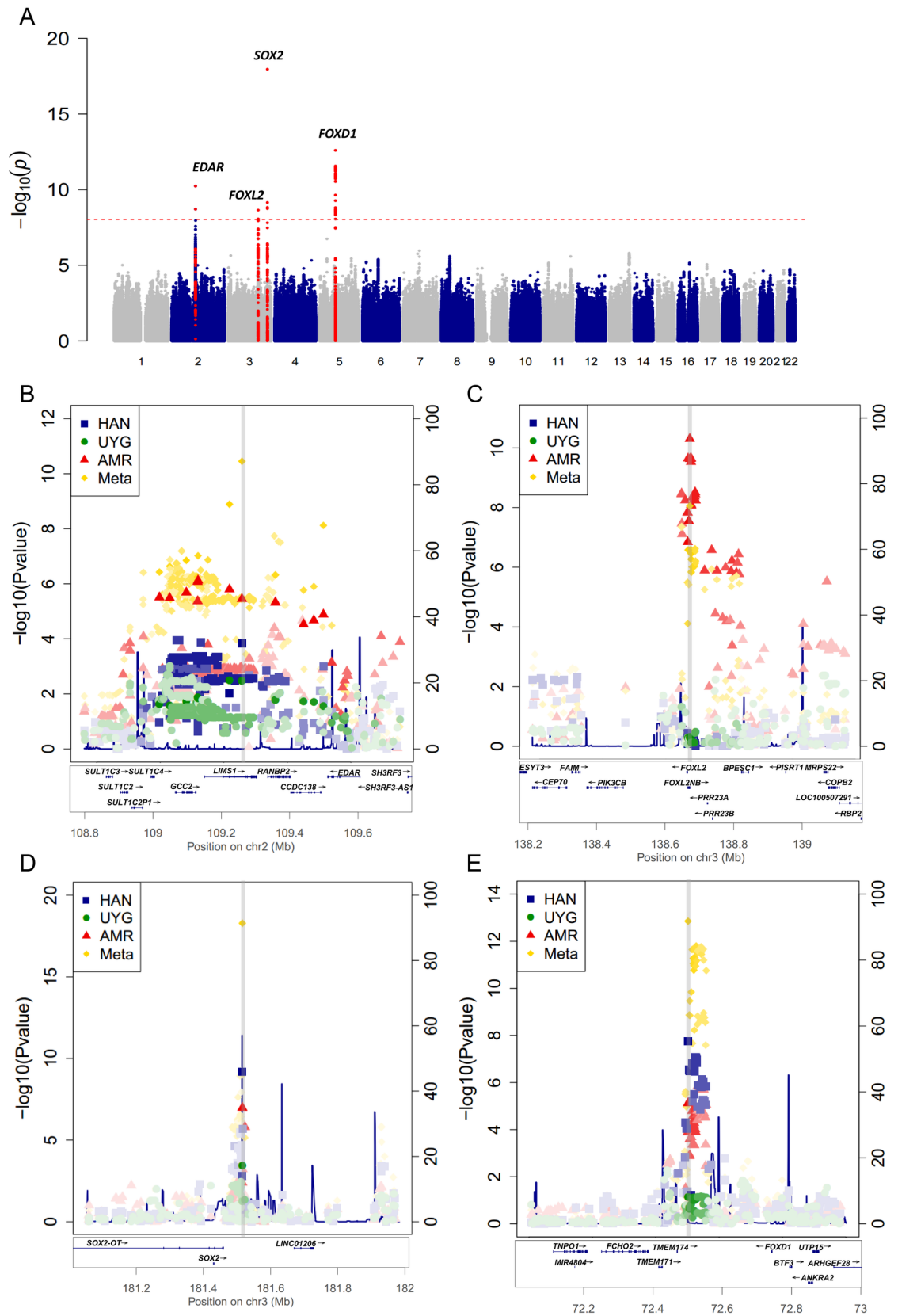


Fig 2. Manhattan plot showing the results of the GWAS meta-analysis for eyebrow thickness in Han Chinese, Uyghurs, and Latin Americans. A) Manhattan plot illustrating results of the transethnic meta-analysis of 2961 Han Chinese, 721 Uyghurs and 2301 Latin Americans. The red line indicates the threshold for genome-wide statistical significance ($P < 5 \times 10^{-8}$). Red dots represent SNPs that are close (< 5 kb) to the genome-wide significant signals. Regional association and linkage disequilibrium plots are shown for the significantly associated regions around B) rs1866188, C) rs112458845, D) rs1345417 and E) rs12651896 (gray bar). Different colors denote different populations. Increasing color intensities represent an increasing degree of linkage disequilibrium (r^2) with the top SNP in each panel. The recombination rate (right-hand y axis) is plotted in blue and is based on the ASN population from the 1000 Genome Project. Exons for each gene are represented by vertical bars below the x axis, based on all isoforms available from the hg19 UCSC Genome Browser.

<https://doi.org/10.1371/journal.pgen.1007640.g002>

Among the genes showing significant changes in expression levels, only *SOX2* and *FOXD1* were reported to be related to hair growth [20,21]. We thus chose to focus on these two genes. For each of the two lenti-Cas9-sgRNAs targeting rs1345417 and rs12651896, we derived multiple independent single cell clones of infected A375 cells and characterized their exact deletion/mutation status at the target SNP sites (S4 Fig). We found that *SOX2* expression was significantly reduced in A375 cell clones carrying deletions/substitutions encompassing rs1345417, in comparison with cells infected with empty lenti-Cas9 vector or with lenti-Cas9-control sgRNA (Fig 4E and 4F). Importantly, A375 cell clones that were infected with rs1345417 targeting lenti-Cas9-sgRNA but where the SNP site was not successfully edited, did not show reduced *SOX2* expression (Fig 4E and 4F). Similarly, *FOXD1* expression was significantly reduced in all A375 cell clones carrying a deletion encompassing the rs12651896 site, compared to both controls and unsuccessfully edited infected cell clones (Fig 4G and 4H). In one clone (896sg1m1), β -actin expression was also unexpectedly reduced, probably due to off-target effects.

To test if a single nucleotide substitution event is sufficient to affect endogenous *SOX2* gene expression, we conducted a CRISPR/Cas9-mediated knock-in experiment at rs1345417, for which native A375 cells are homozygous (G/G). Consistent with our expectations, *SOX2* expression levels were significantly lower in an edited, G/C heterozygous A375 clone than in the original G/G A375 cells (Fig 4I).

Additionally, we conducted a luciferase reporter experiment for the genomic region surrounding rs1345417 (S5 Fig). We found that a 1,495 bp genomic fragment encompassing the rs1345417 site and containing its common G allele can act as a transcriptional enhancer. Its insertion before a *SOX2* promoter sequence led to 3 to 4-fold increase in reporter expression (S5 Fig). Moreover, a G>C mutation at rs1345417 on the reporter construct resulted in significantly reduced reporter activity, in line with our observations in the CRISPR/Cas9 experiments above (Fig 4I). Together, our data indicate that genetic variation at rs1345417 and rs12651896 can affect the transcription of *SOX2* and *FOXD1*, respectively.

Testing for signatures of positive selection in associated regions

For some of the top associated loci, allele frequencies varied among populations (S6 Fig). This variation could be caused either by random genetic drift or by local positive selection. To assess whether positive selection could have helped shape variation in the genomic regions associated with human eyebrow thickness, we applied several statistical genetics methods. Using the Integrated Haplotype Score (iHS) [22] and the Composite of Multiple Signals (CMS) statistic [23], we did not find any evidence indicating that *SOX2*, *FOXD1* and *FOXL2* are subject to positive selection in East Asian (CHB), European (CEU) and African (YRI) populations (S7 and S8 Figs). However, there were highly significant signatures of strong positive selection in the *EDAR* region. This is not surprising, as our top signal near *EDAR* (rs1866188) is in high LD with rs3827760, a strongly selected functional SNP causing a number of ectodermal related phenotypic changes, as demonstrated previously [24]. Therefore, the signal of

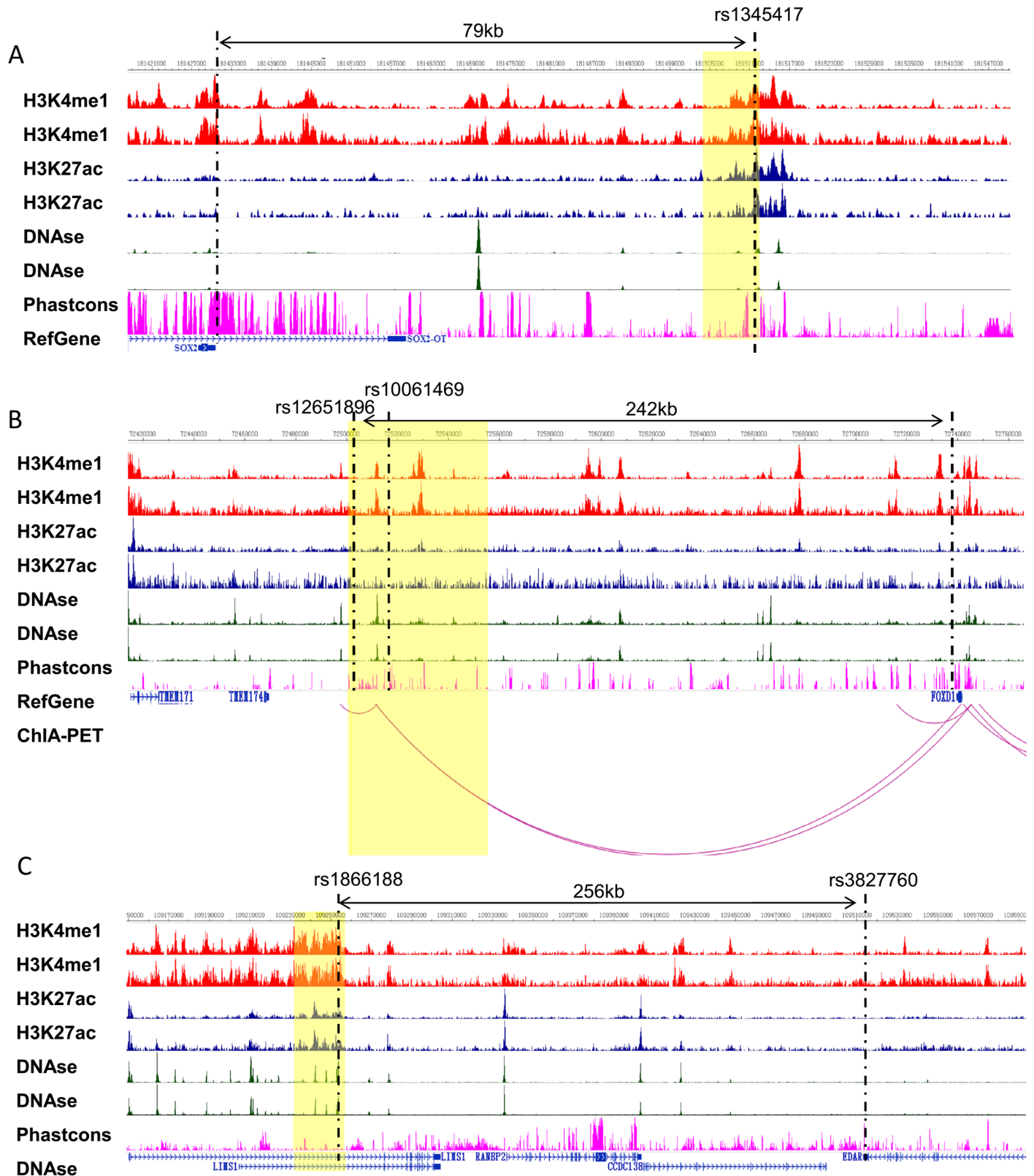


Fig 3. Epigenetic annotation suggests the presence of putative regulatory regions at loci associated with eyebrow thickness. Epigenetic annotation at the significantly associated regions around A) rs1345417 (3q26.33), B) rs12651896 (5q13.2) and C) rs1866188 (2q12.3), based on ENCODE and REMC project data.

Regions of significant association ($P < 5 \times 10^{-8}$) are denoted by a yellow box, with the top signal indicated by a black dashed line. The region exhibits distinct active enhancer signatures defined by epigenetic marks, such as H3K4me1 (red) and H3K27ac (blue) histone modifications and DNase hypersensitivity (green) in foreskin melanocyte primary cells, based on two independent biological replicates. Phastcons (pink) indicates the evolutionary conservation. ChIA-PET indicates long-range chromatin interaction. The different tracks were overlaid with physical positions using the WashU Epigenome Browser.

<https://doi.org/10.1371/journal.pgen.1007640.g003>

selection observed for rs1866188 may well be explained by the selective pressure on rs3827760. To test whether the differences in allele frequencies may stem from different local selection pressures, we applied a probabilistic approach described by He and colleagues [25] to quantify local inter-population differences in selection for the four top loci. Apart from rs1866188 at *EDAR*, we found no significant differences in selection for any other SNP in the associated regions (S9 Fig).

To test whether eyebrow thickness might be subject to polygenic selection, we applied the polygenic scores test developed by Berg and Coop [26]. This test measures the total frequency of associated alleles in a population, weighting each allele by its effect size. Loci that have undergone local positive selection will show greater divergence than expected under the neutral model. Previous studies using this method have found excess variance among populations for genetic scores associated to height, demonstrating that height is subject to local positive selection [27]. Here, we calculated the polygenic score for eyebrow thickness based on the top four associated variants. The resulting scores were similar between populations and showed no excess variance due to positive selection ($P = 0.567$, S10 Fig), indicating that the allele frequency differences observed among populations are better explained by random genetic drift than by selection. Our results thus provide no evidence that eyebrow thickness is under strong positive selection in human populations.

Discussion

Factors associated with eyebrow thickness

We found that eyebrow thickness is significantly associated with age and gender. As may be expected, older adults tend to have a significantly reduced eyebrow thickness due to the weakened biological function of older follicle cells. The eyebrows of males are generally thicker than those of females. Eyebrow plucking is widespread among females and may thus have affected our results; nevertheless, the large and consistent differences observed between genders are likely to be real, considering that androgens tend to stimulate hair growth [28,29].

The top associated SNP at 3q26.33, rs1345417, is located about 80 kb downstream of the *SOX2* gene (Sex Determining Region Y-Box 2), an important transcription factor that is highly expressed in the dermal condensate (DC) and dermal papilla (DP) of growing follicles [30,31]. Interestingly, fine-tuning of *SOX2* expression appears to play an important role in the regulation of hair thickness. In murine skin development, from E18.5 onwards, Sox2 expression becomes confined to DPs in thick guard/awl/auchene hairs, but not in thin zigzag hairs [20]. Moreover, conditional ablation of Sox2 from the DP resulted in significant reduction in the length of awl/auchene, but not zigzag hairs [20]. These findings are consistent with our hypothesis that the G>C mutation at rs1345417 may cause reduced eyebrow thickness by downregulating *SOX2* expression. The top SNP within the second signal at 5q13.2, rs12651896, is located 242 kb downstream of *FOXD1* (Forkhead Box D1). This gene belongs to the forkhead family of transcription factors, whose members are characterized by a distinct forkhead domain. *FOXD1* is especially enriched in DC cells, a precursor of DP/dermal sheath niche cells within the mature follicle [21]. Finally, rs1866188 on chr2q12.3 is located 253 kb upstream of *EDAR* (Ectodysplasin A receptor), a gene which plays an important role in the development of ectodermal tissues such as hair, teeth, and sweat glands [24]. Previous studies

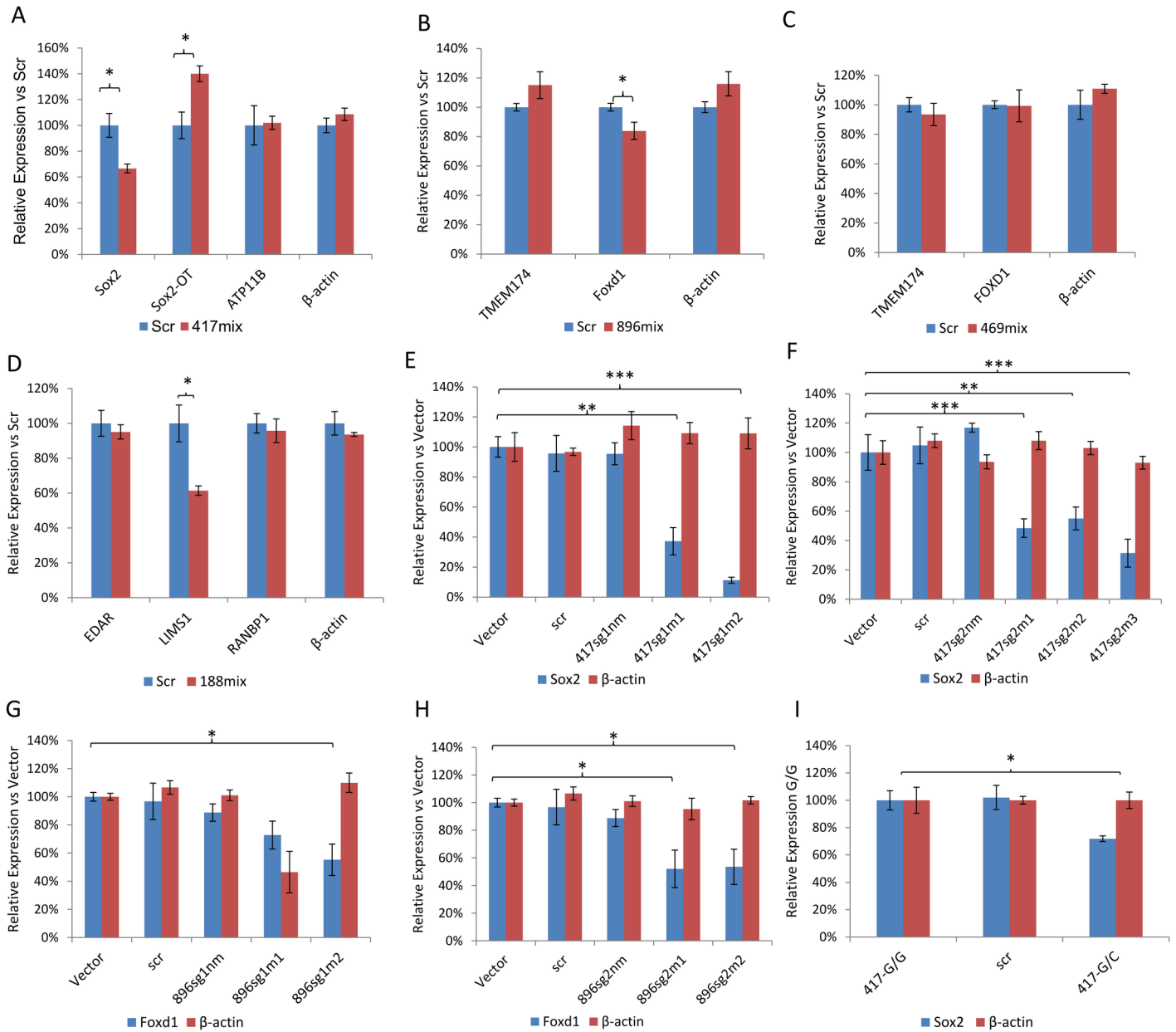


Fig 4. Cas9-mediated gene editing provided evidence that rs1345417 and rs12651896 affect the transcriptional activity of the nearby SOX2 and FOXD1. (A-D) qRT-PCR analysis of relative expression of nearby genes near (A) rs1345417, (B) rs12651896, (C) rs10051469 and (D) rs1866188. Scr denotes lentiCRISPR-Scramble sgRNA infected cells. 417mix, 896mix, 469mix and 188mix denote CRISPR-Cas9 edited mixed clones for rs1345417, rs12651896, rs10051469 and rs1866188, respectively. (E-H) qRT-PCR analysis of relative SOX2 and FOXD1 expression in the CRISPR-Cas9 edited A375 cell clones. Especially, E) 417sg1m1-2: clone 1 and 2 edited by sgRNA1 for rs1345417; F) 417sg2m1-3: clone 1-3 edited by sgRNA2 for rs1345417. G) 896sg1m1-2: clone 1 and 2 edited by sgRNA1 for rs12651896. H) 896sg2m1-2: clone 1-2 edited by sgRNA2 for rs12651896. Detailed DNA sequencing results for each clone are shown in Supplementary Fig 4. Vector (lentiCRISPR vector infected cells), Scr (lentiCRISPR-Scramble sgRNA infected cells), sg1nm and sg2nm (cells infected with lentiCRISPR-sgRNA1 or sgRNA2 but not detectably modified near the rs1345417 and rs12651896 sites). (I) qRT-PCR analysis of relative SOX2 expression in heterozygously edited A375 cell clones, as above. 417-G/G (Original A375 cell line), Scr (lentiCRISPR-Scramble sgRNA infected cells), 417-G/C (the G/C-heterozygous A375 clone) Error bars represent standard errors. *p<0.05, **p<0.01, ***p<0.001, t-test comparing to vector control. N = 3 for each experiment.

<https://doi.org/10.1371/journal.pgen.1007640.g004>

have consistently found *EDAR* to be implicated in beard density [8] and hair thickness [24] and straightness [11,32,33].

Regulatory variants influencing eyebrow thickness

It is notable that all of the signals identified by our GWAS fall into regulatory regions. To date, hundreds of GWAS have been conducted, resulting in the identification of a large number of genetic variants associated with common diseases and phenotypic variation. The majority (~93%) of variants associated with common traits lie within non-coding sequences, complicating their functional evaluation [34]. Recent studies have found that these variants are concentrated in regulatory DNA. This remains true even after adjusting for microarray SNP ascertainment bias and suggests that non-coding variants may act by causing changes in gene expression levels [34], as supported by several lines of evidence [35–39]. The association signals found here at 3q26.33 (rs1345417), 5q13.2 (rs12651896), and 2q12.3 (rs1866188) are all located within active enhancer regions characterized by epigenetic markers, such as H3K4me1 and H3K27ac histone modifications, and DNase hypersensitivity in epithelial cells. Our functional validation experiments provided evidence for enhancer activity around rs1345417 and rs12651896. It is thus highly plausible that these variants affect eyebrow thickness by regulating the expression of *SOX2* and *FOXD1*, respectively. In particular, the CRISPR/Cas9-mediated knock-in experiment provided direct evidence that a single substitution at rs1345417 is sufficient to affect the endogenous gene expression of *SOX2*. Our study represents a successful example of how GWAS and CRISPR/Cas9 technology can be combined to demonstrate the involvement of non-coding variants with regulatory functions in common diseases and normal phenotypic variation.

Population heterogeneity in genes associated with eyebrow thickness

The *FOXL2* variant rs112458845 has previously been found to be associated with eyebrow thickness in Latin Americans. Here, we found no significant evidence of association of this variant with this phenotype in East Asians or Europeans. This may partly be due to the frequency distribution of the minor allele, which is rare in East Asians (4%) and absent in Europeans (0%), but relatively common in Native Americans (26%). Additionally, and perhaps more importantly, allelic effect sizes may be population specific due to a unique yet unidentified environmental or genetic background and may thus vary between Latin Americans on the one hand, and East Asians and Europeans on the other. A similar impact of population heterogeneity on allelic effect sizes has been reported for other traits, such as follicular lymphoma [40], body bone mineral density [41], and Type 1 diabetes [42].

Eyebrow thickness is unlikely to be subject to strong positive selection

It has long been debated whether eyebrow thickness is a selected trait or a ‘neutral feature’ with no apparent link to individual fitness [3,6,7]. We used several methods to detect potential signatures of positive selection for the variants associated with eyebrow thickness. First, we tested whether any of the associated regions overlapped with signals of positive selection. We then used a recently developed probabilistic method to test and estimate differences in selection of the associated variants between populations. We further tested the presence of polygenic selection by examining subtle allele frequency shifts across multiple loci. Previous studies using the above methods have found signatures of positive selection for a range of human traits, including height, skin color, and BMI [23,25,26,43]. However, apart from the *EDAR* region around rs3827760, a SNP known to be under strong selection, we found no significant signatures of positive selection for variants associated with eyebrow thickness. These results suggest that eyebrow thickness may not be subject to strong positive selection, at least not via the genes identified here. In this context, it is worth noting that most studies postulating sexual selection of the eyebrow were based on reconstructed attractiveness [3,5,7], and it

may be argued that the perception of attractiveness can vary significantly over time [3]. Therefore, while sociological studies have indicated that eyebrow thickness may be subject to sexual selection, our study does not provide any support for this conclusion from an evolutionary or genetic perspective.

In conclusion, we identified three novel genetic variants near *SOX2*, *FOXD1* and *EDAR* that influence eyebrow thickness. We demonstrated that rs1345417 and rs12651896 affect the transcriptional activity of the nearby *SOX2* and *FOXD1* genes. Furthermore, we found evidence for population heterogeneity in the genetics of eyebrow thickness. Finally, our results suggest that eyebrow thickness may not be subject to strong positive selection.

Materials and methods

Ethics statement

The Taizhou Longitudinal Study was carried out following protocols approved and oversight by the Institutional Research Board at Fudan University (Ethics Research Approval No.85). The Xinjiang Uyghur Study was conducted with the official approval of the Ethics Committee of the Shanghai Institutes for Biological Sciences (ER-SIBS-261410). The CANDELA ethics approval was obtained from: Universidad Nacional Autonoma de Mexico (Mexico), Universidad de Antioquia (Colombia), Universidad Peruana Cayetano Heredia (Peru), Universidad de Tarapaca (Chile), Universidade Federal do Rio Grande do Sul (Brasil) and University College London (UK, approval number 3351/001). The Rotterdam Study has been approved by the Medical Ethics Committee of the Erasmus MC (registration number MEC 02.1015) and by the Dutch Ministry of Health, Welfare and Sport (Population Screening Act WBO, license number 1071272-159521-PG). All participants provided written informed consent in these four studies.

Populations and samples

This study is based on data from four populations (S1 Table): Han Chinese, Uyghurs, Latin Americans and Europeans. 2,961 Han Chinese (including 1,060 males and 1,901 females, with an age range of 31–87) were enrolled in Taizhou, Jiangsu Province, as part of the Taizhou Longitudinal Study (TZL) [10], in 2014. 721 Uyghurs (including 282 males and 439 females, with an age range of 17–25) were enrolled at Xinjiang Medical University, Urumqi, Xinjiang Province, China, as part of the Xinjiang Uyghur Study (UYG) in 2013–2014. Additionally, we collected summary statistics for a previously conducted GWAS on eyebrow thickness in Latin Americans of the CANDELA cohort, details of which have been previously published [8]. The Rotterdam Study is a population-based prospective study including a main cohort (RS1) and two extensions (RS2 and RS3) [12,13]. All participants were examined in detail at baseline. Collection and purification of DNA have been described in detail previously [12]. The Rotterdam Study has been entered into the Netherlands National Trial Register (NTR; www.trialregister.nl) and into the WHO International Clinical Trials Registry Platform (ICTRP; www.who.int/ictip/network/primary/en/) under shared catalogue number NTR6831. All participants provided written informed consent to participate in the study and to have their information obtained from treating physicians.

Ordinal phenotyping

Eyebrow thickness (i.e., density) was rated by eye on a three-point scale (TZL, UYG, RS: scarce, normal, and dense; CANDELA: low, medium and high), following an established standard and based on photographic imagery (S1 Fig). For the TZL and UYG cohorts, each case

was rated independently by two different investigators. The inter-rater reliability was evaluated with the Kappa statistic. Cases where ratings were inconsistent were reviewed by a third investigator, who made the final decision. For the CANDELA cohort, an interview of the volunteers had indicated that most women modified their eyebrows; in this cohort, eyebrow thickness was therefore only scored in men. Phenotyping was performed by an experienced investigator, and intra-rater reliability was assessed for 150 individuals. For RS, three investigators simultaneously and independently evaluated all photos, which were displayed on two identical screens with the same settings. Before evaluation, a total of 50 photos were openly discussed to reach a consensus between the three investigators. Inter-rater reliability was also evaluated with the Kappa statistic. The average score from the three independent ratings was used as the final phenotype in all subsequent analysis.

Genotype quality control and imputation

For TZL and UYG, blood samples were collected, and DNA was extracted. All samples were genotyped using the Illumina HumanOmniZhongHua-8 chip, which interrogates 894,517 SNPs. To control for genotype quality, we used PLINK 1.9 [44] to exclude individuals with more than 5% missing data, related individuals, and those that failed the X-chromosome sex concordance check, or for whom the available information on ethnicity was incompatible with their genetic information. We also excluded SNPs with more than 2% missing data, with a minor allele frequency (MAF) below 1%, and those that failed the test for Hardy-Weinberg equilibrium ($P < 1 \times 10^{-5}$). The chip genotype data were phased using SHAPEIT [45], and IMPUTE2 [46] was then used to impute genotypes at non-genotyped SNPs using variant positions from the 1000 Genomes Phase 3 data as a reference. SNPs with an imputation quality score (INFO) below 0.8 or a MAF below 1% were eliminated from further analyses. For the Han Chinese population, a total of 6,343,243 imputed SNPs passed quality control and were combined with 776,213 genotyped SNPs for association analysis. For the Uyghur population, a total of 6,414,304 imputed SNPs passed quality control and were combined with 810,648 genotyped SNPs for further analyses. In RS1 and RS2, genotyping was carried out using the Infinium II HumanHap550K Genotyping Bead Chip version 3, which contains 6,787,905 probes. Complete information on genotyping protocols and quality control measures for RS1 and RS2 have been described previously [47,48]. In RS3, genotyping methods closely followed those established for RS1 and RS2, but a denser array, the Human 610 Quad Arrays of Illumina with 15,880,747 probes, was used. Individuals with a call rate $< 97.5\%$, gender mismatch with typed X-linked markers, or excess autosomal heterozygosity (> 0.33) were excluded, as were duplicates or 1st degree relatives identified using IBS probabilities, and outliers using multi-dimensional scaling analysis with reference to the 210 Hap Map samples. Genome-wide imputation in RS3 closely followed the methods used in RS1 and RS2, as described in detail previously [48]. Genotypes were imputed using MACH [49] based on phased autosomal chromosomes of the 1000 Genome reference panel, orientated on the positive strand.

Population stratification analysis

The effects of possible population stratification were corrected using the EIGENSTRAT [50] tool from the EIGENSOFT package. To this end, TZL and UYG data were combined with 1000 Genomes Phase 3 data for YRI, CHB and CEU populations. 102,284 SNPs in low linkage equilibrium ($r^2 < 0.2$) were selected for analysis. Principal component (PC) analysis did not find any outliers in TZL and UYG (S11 Fig).

Statistical genetics analyses

Initial genome-wide association tests using multiple linear regression with an additive genetic model incorporating gender, age and four genetic PCs as covariates were performed in PLINK 1.9 [44]. Expected and observed association results for all tests were visualized in quantile-quantile (Q-Q) plots to assess systematic inflation in association resulting from population stratification or other systematic causes of bias. None of the Q-Q plots showed any sign of inflation, the genomic control factor λ being < 1.06 in all cases (S3 Fig). To evaluate the presence of additional independent signals at each locus, we performed conditional analyses by adding the dosages of the top SNP at each locus to the regression model. Q-Q, Manhattan and regional association plots [51] were created in R. The proportion of variance in eyebrow thickness explained by the genetic variants identified was estimated using GCTA [52]. The meta-analysis of the TZL, UYG and CANDELA data sets was performed using METAL [53]. Heterogeneity of SNP associations across studies was tested via Cochran's Q statistic [54], and its magnitude was expressed by I^2 . For SNPs with significant heterogeneity, a random effects model was applied for meta-analysis using METASOFT [55].

Fine mapping and credible set construction

We performed fine mapping of each locus for a 1 Mb genomic interval flanking the top SNP (500 kb upstream and 500 kb downstream) using PAINTOR [14,15]. For each SNP within this 1 Mb region, the posterior probability that this SNP is driving the region's association signal was calculated by dividing the SNP's Bayes factor (BF) by the sum of the BFs of all SNPs in the region [56]. A 99% credible set was then constructed by (1) ranking all variants according to their Bayes factor, and (2) including ranked variants until their cumulative posterior probability of representing the causal variant at a given locus exceeded 0.99 [57].

Functional annotation

To further facilitate the prioritization of variants for functional analysis, we used CADD [16] (Combined Annotation-Dependent Depletion) and DeepSEA [17] (deep learning-based sequence analyzer) to evaluate the possible functional consequences of the variants in the 99% credible set.

Candidate gene identification and regulatory annotation

Candidate genes were chosen based on their distance to the associated loci as well as their function, involvement in biochemical pathways, tissue expression, and involvement in similar phenotypes. The relevant information was obtained from NCBI [58] and Ensemble [59], as well as available published data. We used HaploReg v4.1 [60] to extract a variety of regulatory annotations, including histone modification (ChIP-seq tracks), chromatin state segmentations (15-state) and ChIA-PET [61] (Chromatin Interaction) from ENCODE [18] and the Roadmap Epigenomics Project [19], conserved regions from GERP [62] and Phastcons [63], and eQTLs from the GTEx [64] and GEUVADIS databases [65].

Cell culture

No cell lines were found in the database of commonly misidentified cell lines maintained by ICLAC and NCBI Biosample. Cell lines were not authenticated. NHEM (human melanocytes) and A375 (human melanoma) were purchased from the cell bank of the Chinese Academy of Sciences. HACAT (immortal keratinocytes) and SCC13 (skin squamous-cell carcinoma cell

line) were purchased from ATCC. Cell lines were routinely tested for mycoplasma infection. Cells were cultured using DMEM+10%FBS+1%Penicillin-Streptomycin.

Plasmid construction and luciferase assays

A 1,495 bp genomic fragment comprising the rs1345417 enhancer was amplified from human genomic DNA and cloned into a pGL3-promoter vector, in which the SV40 promoter was replaced by a SOX2 promoter. The G>C mutation was introduced by site-directed mutagenesis (Takara). The inserts in each construct were verified by sequencing. The detail information of primer sequences can be found in [S5 Table](#). Constructs were transfected with equimolar amounts (500 ng) of luciferase reporter plasmids into A375 Melanoma cells using jetPEI (Polyplus), according to the manufacturer's instructions. Luciferase expression was normalized to 200 ng Renilla luciferase expression (pRL-SV40). Cells were harvested after 48 h. Luminescence activity was measured with a Berthold Centro LB 960 Microplate Luminometer. Data represent at least three independent experiments. Student's two-tailed t-test was used to determine statistical significance.

CRISPR/Cas9-mediated gene editing

For each candidate variant, two sgRNAs were designed, cloned into the lentiCRISPR v2 vector, and packaged into lentivirus as previously described [66]. sgRNAs used for rs1345417: sgRNA1 (CCTGCTTTTGCCTCAGCCCACAT) and sgRNA2 (CCCACATCTTCTCTATTAGTAAG). sgRNAs used for rs12651896: sgRNA1 (CAAAATGTTCTTGCTAGCATATCCA) and sgRNA2 (GCATATCCATAACTAGCACAGG). sgRNAs used for rs10061469: sgRNA1 (ACAACCTGC AATAAACTATTAA). sgRNAs for rs1866188 site: sgRNA1 (GAGTGGCCACTCTCTTTTGC) and sgRNA2 (GAATGCATAAGGA TCAAATCG). Scramble Control sgRNA sequence is (CCCACATAGTCTCACTTAG TAAG).

For target site deletion via lentiCRISPR-sgRNA virus infection, stably infected cells were selected on puromycin. For clone selection, stably infected cells were diluted to allow colonial growth. Single colonies were individually picked for DNA sequencing of the target site. Because protospacer adjacent motives were located as far as 100 bp upstream and 22 bp downstream, the deletion at rs1866188 was considerably larger than for the other sites.

For G>C substitution at rs1345417 in A375 cells, we used a CRISPR-Cas9 mediated knock-in strategy. Specifically, in order to substitute the G/G of rs1345417 in A375 cell, a ~1000bp DNA fragment encompassing the rs1345417 site from a Chinese individual with a C/C homozygote genotype was PCR amplified and TA cloned into the pMD18T Vector (Takara) to construct a C-donor plasmid. We then co-transfected the C-donor plasmid and the lenticrispr-rs1345417-sgRNA2 plasmid into A375 cells using the Effectene reagent (Qiagen). 48 h after transfection, the cells were selected on puromycin for 48 h to eliminate untransfected cells. Successfully transfected cells were then diluted for colonial growth. Single colonies were individually picked for DNA sequencing to screen for substitution at the target site. In total, 44 clones were screened.

Molecular biology

Sequencing of the rs1345417 site: Genomic DNA was extracted from each cell clone using ZR Genomic DNA-tissue MiniPrep (Zymo) following the manufacturer's protocol. The rs1345417 genomic region was amplified from genomic DNA by nested PCR and TA-cloned into pMD18 T vector for sequencing. At least four individual TA-clones were sequenced for each cell clone. RNA extraction was conducted using Direct-zol RNA MiniPrep Plus (Zymo) following the manufacturer's protocol. Reverse transcription was conducted using the iscript

cDNA synthesis kit (Biorad) following the manufacturer’s protocol. Real-time PCR experiments were conducted on a VIIA7 Fast Real-Time PCR system (Applied Biosystem) using the iTaq universal SYBR Green supermix (Biorad). All statistical analyses were conducted using Microsoft Excel and the GraphPad Prism 6 software.

Tests for positive selection

Genomic characteristics resulting from strong recent positive selection include low haplotype diversity and high linkage disequilibrium. We calculated extended haplotype homozygosity (EHH) [22,67] for all SNPs until $EHH < 0.05$ in CEU, CHB and UYG samples. Next, the integrated haplotype score (iHS) [68] was calculated for all SNPs, with an allele frequency bin of 0.05 to standardize iHS scores against other SNPs of the same frequency class within the region. Finally, we calculated P values assuming a Gaussian distribution of iHS scores under the neutral model, which was checked by plotting the values against a Gaussian distribution. The empirical significance cutoff was based on the top 0.1% iHS scores. We also performed genome-wide CMS [23] analysis in African (YRI), European (CEU), and East Asian (JPT +CHB) populations from the 1000 Genome Project [69] to validate our results. The empirical significance cutoff was based on the top 0.1% CMS scores. Differences in allele frequencies are indicators of possible differences in selection between populations. To test whether the differences in allele frequencies may result from different local selection pressure, we used a probabilistic method which was recently put forward by He and colleagues [25]. We used this approach to test and estimate selection differences between populations for the four top associated loci. We first estimated differences in selection coefficients between populations (CHB, CEU and YRI) using logarithmic odds ratios of allele frequencies. The variance of the estimation was then calculated based on genome-wide variants. Finally, we calculated P values assuming a Gaussian distribution of the statistic under the neutral model. The significance cutoff was $P < 0.005$ after multiple testing correlation.

To investigate whether the loci associated with eyebrow thickness are more differentiated among populations than expected under neutral genetic drift, for each population m , we calculated the polygenic eyebrow thickness score (genetic score) as

$$Z_m = 2 \sum_{i=1}^L \beta_i p_{mi}$$

where β_i is the effect size of the eyebrow thickness increasing allele l , and p_{mi} is the frequency of allele l in population m . We first used the four loci identified here in conjunction with allele frequency data from the 1000 Genome Project dataset to estimate the genetic score for eyebrow thickness in each population, with the effect sizes estimated in the meta-analysis. To test whether there was a signature of polygenic adaptation, we then adopted a framework developed by Berg and Coop [26], which builds a multivariate normal model based on matched, presumably neutral variants, to account for relationships among populations. Traits that have undergone local selection will show excess divergence among populations (significance cutoff: $P < 0.05$).

Supporting information

S1 Fig. Representative images of eyebrow thickness. Level 1 (scarce): low eyebrow density, the brow does not cover the skin completely. Level 2 (normal): the eyebrow covers the skin, there is no hair between the two brows. Level 3 (dense): high eyebrow density, the color of the

eyebrow is darker than for level 2.
(PNG)

S2 Fig. Manhattan plot showing the results of the GWAS for eyebrow thickness in the Uyghurs. Manhattan plot illustrating the results of the genome-wide scan for eyebrow thickness in 721 Uyghurs after adjusting for the top four PCs, gender and age. The red line indicates the threshold for genome-wide statistical significance ($P < 5 \times 10^{-8}$).
(PNG)

S3 Fig. Quantile-Quantile (Q-Q) plots for the four GWAS included in this study. a) TZL, b) UYG, c) CANDELA and d) meta-analysis.
(PNG)

S4 Fig. CRISPR/Cas9-mediated deletion in the human A375 cell line. DNA sequences of the regions around a) rs1345417, b) rs12651896, c) rs10061469 and d) rs1866188 in original A375 cells and their CRISPR-Cas9 edited clones. For rs1345417, 417sg1m1-2: clone 1 and 2 edited by sgRNA1. 417sg2m1-3: clone 1–3 edited by sgRNA2. 417-G/C: a single nucleotide substitution event. For rs12651896, 896sg1m1-2: clone 1 and 2 edited by sgRNA1. 896sg2m1-2: clone 1–2 edited by sgRNA2. For rs1866188, clone 1 and 2 edited by both sgRNA1 and sgRNA2.
(PNG)

S5 Fig. Luciferase reporter assays linking rs1345417 to altered levels of gene expression. A) Schematic diagram of the constructed luciferase reporters. Triangles and green rectangles represent the promoter and luciferase gene, respectively. The putative regulatory element (1,495-bp insertion) is indicated by yellow rectangles, with the SNP rs1345417 represented as a red line (G>C). pGL3-Basic, empty vector (SV40 promoter); SOX2-Pro, vector containing the SOX2 promoter; SOX2-G, G allele at rs1345417; SOX2-C, C allele at rs1345417. B-D) Three repeats of luciferase reporters in human A375 cells. Bars represent the mean intensity of luciferase gene activity relative to the empty vector (pGL3-Basic) as a control, measured 48h after transfection for a typical experiment. Error bars represent standard errors. * $p < 0.05$, ** $p < 0.01$, *** $p < 0.001$, t-test comparing to vector control. N = 3 for each experiment.
(PNG)

S6 Fig. Geographical distribution of the minor allele frequencies for the significant variants identified here, based on the Human Genome Diversity Project. Allele frequency data from 53 world-wide populations were taken from the Human Genome Diversity Project. For a) rs1345417, b) rs12651896 and c) rs1866188, ancestral alleles are represented in blue, derived alleles in orange.
(PNG)

S7 Fig. Results of the selection analysis on EDAR, FOXL2, SOX2 and FOXD1 based on CMS scores. CMS scores are plotted against physical distance for a) EDAR, b) FOXL2, c) SOX2 and d) FOXD1 regions in CEU, CHB+JPT and YRI populations. The yellow line marks the location of the index SNP in each region (Table 1). The black dashed line indicates the threshold of top 0.1% chromosome-wide CMS scores (> 4.8).
(PNG)

S8 Fig. Results of the selection analysis on EDAR, FOXL2, SOX2 and FOXD1 based on iHS scores. Absolute iHS scores are plotted against physical distance for a) EDAR, b) FOXL2, c) SOX2 and d) FOXD1 regions in CEU, CHB+JPT and YRI populations. The yellow line marks the location of the index SNP in each region (Table 1). The black dashed line indicates the

threshold of top 0.1% chromosome-wide iHS scores (>3.1).
(PNG)

S9 Fig. Differences in selection coefficients between populations. The forest plot illustrates the differences in selection coefficients of variants in four independent genomic signals for eyebrow thickness. Differences are shown between three 1000 Genomes populations (CEU, CHB, YRI). For each variant, points (and error bars) indicate the estimated differences in selection coefficients (and 99.5% confidence intervals; after multiple testing). Each population pair is denoted by a different color. The underlying data were obtained from phase 3 of the 1000 Genomes Project.
(PNG)

S10 Fig. Visual representation of polygenic selection for eyebrow thickness. The genetic score was calculated on the basis of the four associated variants, with effect sizes estimated in the meta-analysis and allele frequencies obtained from phase 3 of the 1000 Genomes Project.
(PNG)

S11 Fig. Principle component analysis of individuals from Han Chinese, Uyghur and 1000 Genome Project samples. Principal component analysis of 102,284 SNPs ($r^2 < 0.2$) in Han Chinese ($n = 2961$), Uyghurs ($n = 721$), and three 1000 Genome population samples (97 CHB, 86 CEU and 88 YRI) placed Han Chinese and Uyghurs into distinct clusters. There were no significant population outliers in our samples.
(PNG)

S1 Table. Sample phenotype information.
(DOCX)

S2 Table. Phenotyping concordance between cohorts.
(DOCX)

S3 Table. Meta-analysis results for index SNPs.
(DOCX)

S4 Table. Posterior probability and functional annotation of variants at associated loci.
(DOCX)

S5 Table. Primer sequences for plasmid construction and luciferase assays.
(DOCX)

Acknowledgments

We thank all the study participants, the staff from the Taizhou Longitudinal Study and Xinjiang Uyghur Study. We thank Dida Biotech performed the Luciferase assay experiments. We thank Barbara Kremeyer for her insightful revisions on the manuscript. The CANDELA work thank Alvaro Alvarado, Mónica Ballesteros Romero, Mari-Wyn Burley, Ricardo Cebrecos, Debajyoti Choudhury, Miguel Ángel Contreras Sieck, Francisco de Ávila Becerril, Joyce De la Piedra, María Teresa Del Solar, Paola Everardo Martínez, William Flores, Martha Granados Riveros, Wendy Hart, Ilich Jafet Moreno, Jodie Lampert, Mowmita Basak Mow, Paola León-Mimila, Javier Mendoza, Francisco Quispealaya, Diana Rogel Diaz, Ruth Rojas, Norman Russell, Vanessa Sarabia, and Fabienne Tessiot for assistance with volunteer recruitment, sample processing and data entry. We are very grateful to the institutions that kindly provided facilities for the assessment of volunteers, including: Escuela Nacional de Antropología e Historia and Universidad Nacional Autónoma de México (Mexico); Pontificia Universidad Católica

del Perú, Universidad de Lima and Universidad Nacional Mayor de San Marcos (Peru). The Rotterdam Study thank Pascal Arp, Mila Jhamai, Marijn Verkerk, Lizbeth Herrera and Marjolein Peters, PhD, and Carolina Medina-Gomez, MSc, for their help in creating the GWAS database, and Karol Estrada, PhD, Yurii Aulchenko, PhD, and Carolina Medina-Gomez, MSc, for the creation and analysis of imputed data. The authors are grateful to the study participants, the staff from the Rotterdam Study and the participating general practitioners and pharmacists.

Author Contributions

Conceptualization: Liang Zhang, Li Jin, Sijia Wang.

Data curation: Sijie Wu, Manfei Zhang, Xinzhou Yang, Fuduan Peng, Juan Zhang, Jingze Tan, Yajun Yang, Qianqian Peng, Jinxi Li, Yu Liu, Yaqun Guan, Chen Chen, Merel A. Hamer, Changqing Zeng, Kaustubh Adhikari, Carla Gallo, Lavinia Schuler-Faccini, Fan Liu, Manfred Kayser, Andres Ruiz-Linares, Kun Tang, Shuhua Xu, Liang Zhang, Li Jin, Sijia Wang.

Formal analysis: Sijie Wu, Manfei Zhang, Xinzhou Yang, Fuduan Peng, Lina Wang, Yanan Hu.

Funding acquisition: Changqing Zeng, Giovanni Poletti, Rolando González-José, Fan Liu, Manfred Kayser, Andres Ruiz-Linares, Kun Tang, Shuhua Xu, Liang Zhang, Li Jin, Sijia Wang.

Resources: Tamar Nijsten, Giovanni Poletti, Lavinia Schuler-Faccini, Maria-Cátira Bortolini, Samuel Canizales-Quinteros, Francisco Rothhammer, Gabriel Bedoya, Rolando González-José, Hui Li, Jean Krutmann, Fan Liu, Manfred Kayser, Andres Ruiz-Linares, Kun Tang, Shuhua Xu, Liang Zhang, Li Jin, Sijia Wang.

Supervision: Liang Zhang, Sijia Wang.

Writing – original draft: Sijie Wu, Manfei Zhang, Liang Zhang, Sijia Wang.

Writing – review & editing: Kaustubh Adhikari, Fan Liu, Manfred Kayser, Andres Ruiz-Linares.

References

1. Bradley BJ, Mundy NI (2008) The primate palette The evolution of primate coloration, *Evolutionary Anthropology: Issues, News, and Reviews* Volume 17, Issue 2. *Evol Anthropol* 17: 97–111.
2. Jablonski NG (2010) The Naked Truth Recent findings lay bare the origins of human hairlessness-and hint that naked skin was a key factor in the emergence of other human traits. *Scientific American* 302: 42–49.
3. Feser DK, Grundl M, Eisenmann-Klein M, Prantl L (2007) Attractiveness of eyebrow position and shape in females depends on the age of the beholder. *Aesthetic Plastic Surgery* 31: 154–160. <https://doi.org/10.1007/s00266-006-0149-x> PMID: 17235461
4. Knize DM (2007) The importance of the retaining ligamentous attachments of the forehead for selective eyebrow reshaping and forehead rejuvenation. *Plastic And Reconstructive Surgery* 119: 1119–1120. <https://doi.org/10.1097/01.prs.0000253441.51529.83> PMID: 17312534
5. Li YJ, Li HJ, Cai Z (2013) Human eyebrow recognition in the matching-recognizing framework. *Computer Vision And Image Understanding* 117: 170–181.
6. Sadr J, Jarudi I, Sinha P (2003) The role of eyebrows in face recognition. *Perception* 32: 285–293. <https://doi.org/10.1068/p5027> PMID: 12729380
7. Bovet J, Barthes J, Durand V, Raymond M, Alvergne A (2012) Men's Preference for Women's Facial Features: Testing Homogamy and the Paternity Uncertainty Hypothesis. *Plos One* 7.

8. Adhikari K, Fontanil T, Cal S, Mendoza-Revilla J, Fuentes-Guajardo M, et al. (2016) A genome-wide association scan in admixed Latin Americans identifies loci influencing facial and scalp hair features. *Nat Commun* 7: 10815. <https://doi.org/10.1038/ncomms10815> PMID: 26926045
9. Pelletier AT, Few JW (2010) Eyebrow and Eyelid Dimensions: An Anthropometric Analysis of African Americans and Caucasians. *Plastic And Reconstructive Surgery* 125: 1293–1294. <https://doi.org/10.1097/PRS.0b013e3181d45adb> PMID: 20335885
10. Wang XF, Lu M, Qian J, Yang YJ, Li SL, et al. (2009) Rationales, design and recruitment of the Taizhou Longitudinal Study. *Bmc Public Health* 9.
11. Wu S, Tan J, Yang Y, Peng Q, Zhang M, et al. (2016) Genome-wide scans reveal variants at EDAR predominantly affecting hair straightness in Han Chinese and Uyghur populations. *Hum Genet* 135: 1279–1286. <https://doi.org/10.1007/s00439-016-1718-y> PMID: 27487801
12. Hofman A, Grobbee DE, Dejong PTVM, Vandenouweland FA (1991) Determinants Of Disease And Disability In the Elderly—the Rotterdam Elderly Study. *European Journal Of Epidemiology* 7: 403–422. PMID: 1833235
13. Hofman A, Brusselle GGO, Murad SD, van Duijn CM, Franco OH, et al. (2015) The Rotterdam Study: 2016 objectives and design update. *European Journal Of Epidemiology* 30: 661–708. <https://doi.org/10.1007/s10654-015-0082-x> PMID: 26386597
14. Kichaev G, Yang WY, Lindstrom S, Hormozdiari F, Eskin E, et al. (2014) Integrating functional data to prioritize causal variants in statistical fine-mapping studies. *PLoS Genet* 10: e1004722. <https://doi.org/10.1371/journal.pgen.1004722> PMID: 25357204
15. Kichaev G, Pasaniuc B (2015) Leveraging Functional-Annotation Data in Trans-ethnic Fine-Mapping Studies. *Am J Hum Genet* 97: 260–271. <https://doi.org/10.1016/j.ajhg.2015.06.007> PMID: 26189819
16. Kircher M, Witten DM, Jain P, O’Roak BJ, Cooper GM, et al. (2014) A general framework for estimating the relative pathogenicity of human genetic variants. *Nat Genet* 46: 310–315. <https://doi.org/10.1038/ng.2892> PMID: 24487276
17. Zhou J, Troyanskaya OG (2015) Predicting effects of noncoding variants with deep learning-based sequence model. *Nat Methods* 12: 931–934. <https://doi.org/10.1038/nmeth.3547> PMID: 26301843
18. Birney E, Stamatoyannopoulos JA, Dutta A, Guigo R, Gingeras TR, et al. (2007) Identification and analysis of functional elements in 1% of the human genome by the ENCODE pilot project. *Nature* 447: 799–816. <https://doi.org/10.1038/nature05874> PMID: 17571346
19. Kundaje A, Meuleman W, Ernst J, Bilenky M, Yen A, et al. (2015) Integrative analysis of 111 reference human epigenomes. *Nature* 518.
20. Clavel C, Grisanti L, Zemla R, Rezza A, Barros R, et al. (2012) Sox2 in the Dermal Papilla Niche Controls Hair Growth by Fine-Tuning BMP Signaling in Differentiating Hair Shaft Progenitors. *Developmental Cell* 23: 981–994. <https://doi.org/10.1016/j.devcel.2012.10.013> PMID: 23153495
21. Sennett R, Wang ZC, Rezza A, Grisanti L, Roitershtein N, et al. (2015) An Integrated Transcriptome Atlas of Embryonic Hair Follicle Progenitors, Their Niche, and the Developing Skin. *Developmental Cell* 34: 577–591. <https://doi.org/10.1016/j.devcel.2015.06.023> PMID: 26256211
22. Voight BF, Kudravalli S, Wen XQ, Pritchard JK (2006) A map of recent positive selection in the human genome. *Plos Biology* 4: 446–458.
23. Grossman SR, Shylakhter I, Karlsson EK, Byrne EH, Morales S, et al. (2010) A Composite of Multiple Signals Distinguishes Causal Variants in Regions of Positive Selection. *Science* 327: 883–886. <https://doi.org/10.1126/science.1183863> PMID: 20056855
24. Kamberov YG, Wang SJ, Tan JZ, Gerbault P, Wark A, et al. (2013) Modeling Recent Human Evolution in Mice by Expression of a Selected EDAR Variant. *Cell* 152: 691–702. <https://doi.org/10.1016/j.cell.2013.01.016> PMID: 23415220
25. He YG, Wang MX, Huang X, Li R, Xu HY, et al. (2015) A probabilistic method for testing and estimating selection differences between populations. *Genome Research* 25: 1903–1909. <https://doi.org/10.1101/gr.192336.115> PMID: 26463656
26. Berg JJ, Coop G (2014) A Population Genetic Signal of Polygenic Adaptation. *Plos Genet* 10.
27. Robinson MR, Hemani G, Medina-Gomez C, Mezzavilla M, Esko T, et al. (2015) Population genetic differentiation of height and body mass index across Europe. *Nat Genet* 47: 1357–+. <https://doi.org/10.1038/ng.3401> PMID: 26366552
28. Randall VA (2008) Androgens and hair growth. *Dermatologic Therapy* 21: 314–328. <https://doi.org/10.1111/j.1529-8019.2008.00214.x> PMID: 18844710
29. Thornton MJ, Messenger AG, Elliott K, Randall VA (1991) Effect Of Androgens on the Growth Of Cultured Human Dermal Papilla Cells Derived From Beard And Scalp Hair-Follicles. *Journal Of Investigative Dermatology* 97: 345–348. PMID: 2071943

30. Sennett R, Wang Z, Rezza A, Grisanti L, Roitershtein N, et al. (2015) An Integrated Transcriptome Atlas of Embryonic Hair Follicle Progenitors, Their Niche, and the Developing Skin. *Dev Cell* 34: 577–591. <https://doi.org/10.1016/j.devcel.2015.06.023> PMID: 26256211
31. Grisanti L, Clavel C, Cai X, Rezza A, Tsai SY, et al. (2013) Tbx18 targets dermal condensates for labeling, isolation, and gene ablation during embryonic hair follicle formation. *J Invest Dermatol* 133: 344–353. <https://doi.org/10.1038/jid.2012.329> PMID: 22992803
32. Tan JZ, Yang YJ, Tang K, Sabeti PC, Jin L, et al. (2013) The adaptive variant EDARV370A is associated with straight hair in East Asians. *Human Genetics* 132: 1187–1191. <https://doi.org/10.1007/s00439-013-1324-1> PMID: 23793515
33. Peng QQ, Li JX, Tan JZ, Yang YJ, Zhang MF, et al. (2016) EDARV370A associated facial characteristics in Uyghur population revealing further pleiotropic effects. *Hum Genet* 135: 99–108. <https://doi.org/10.1007/s00439-015-1618-6> PMID: 26603699
34. Maurano MT, Humbert R, Rynes E, Thurman RE, Haugen E, et al. (2012) Systematic Localization of Common Disease-Associated Variation in Regulatory DNA. *Science* 337: 1190–1195. <https://doi.org/10.1126/science.1222794> PMID: 22955828
35. Guenther CA, Tasic B, Luo LQ, Bedell MA, Kingsley DM (2014) A molecular basis for classic blond hair color in Europeans. *Nat Genet* 46: 748–752. <https://doi.org/10.1038/ng.2991> PMID: 24880339
36. Pomerantz MM, Ahmadiyeh N, Jia L, Herman P, Verzi MP, et al. (2009) The 8q24 cancer risk variant rs6983267 shows long-range interaction with MYC in colorectal cancer. *Nat Genet* 41: 882–884. <https://doi.org/10.1038/ng.403> PMID: 19561607
37. Musunuru K, Strong A, Frank-Kamenetsky M, Lee NE, Ahfeldt T, et al. (2010) From noncoding variant to phenotype via SORT1 at the 1p13 cholesterol locus. *Nature* 466: 714–U712. <https://doi.org/10.1038/nature09266> PMID: 20686566
38. Degner JF, Pai AA, Pique-Regi R, Veyrieras JB, Gaffney DJ, et al. (2012) DNase I sensitivity QTLs are a major determinant of human expression variation. *Nature* 482: 390–394. <https://doi.org/10.1038/nature10808> PMID: 22307276
39. Oh J, Byrd AL, Park M, Program NCS, Kong HH, et al. (2016) Temporal Stability of the Human Skin Microbiome. *Cell* 165: 854–866. <https://doi.org/10.1016/j.cell.2016.04.008> PMID: 27153496
40. Smedby KE, Foo JN, Skibola CF, Darabi H, Conde L, et al. (2011) GWAS of Follicular Lymphoma Reveals Allelic Heterogeneity at 6p21.32 and Suggests Shared Genetic Susceptibility with Diffuse Large B-cell Lymphoma. *Plos Genetics* 7.
41. Medina-Gomez C, Kemp JP, Estrada K, Eriksson J, Liu J, et al. (2012) Meta-Analysis of Genome-Wide Scans for Total Body BMD in Children and Adults Reveals Allelic Heterogeneity and Age-Specific Effects at the WNT16 Locus. *Plos Genetics* 8.
42. Maier LM, Lowe CE, Cooper J, Downes K, Anderson DE, et al. (2009) IL2RA Genetic Heterogeneity in Multiple Sclerosis and Type 1 Diabetes Susceptibility and Soluble Interleukin-2 Receptor Production. *Plos Genetics* 5.
43. Liu X, Ong RT, Pillai EN, Elzein AM, Small KS, et al. (2013) Detecting and characterizing genomic signatures of positive selection in global populations. *Am J Hum Genet* 92: 866–881. <https://doi.org/10.1016/j.ajhg.2013.04.021> PMID: 23731540
44. Purcell S, Neale B, Todd-Brown K, Thomas L, Ferreira MA, et al. (2007) PLINK: a tool set for whole-genome association and population-based linkage analyses. *Am J Hum Genet* 81: 559–575. <https://doi.org/10.1086/519795> PMID: 17701901
45. Delaneau O, Marchini J, Zagury JF (2012) A linear complexity phasing method for thousands of genomes. *Nature Methods* 9: 179–181.
46. Howie BN, Donnelly P, Marchini J (2009) A Flexible and Accurate Genotype Imputation Method for the Next Generation of Genome-Wide Association Studies. *Plos Genetics* 5.
47. Estrada K, Krawczak M, Schreiber S, van Duijn K, Stolk L, et al. (2009) A genome-wide association study of northwestern Europeans involves the C-type natriuretic peptide signaling pathway in the etiology of human height variation. *Human Molecular Genetics* 18: 3516–3524. <https://doi.org/10.1093/hmg/ddp296> PMID: 19570815
48. Liu F, Wollstein A, Hysi PG, Ankra-Badu GA, Spector TD, et al. (2010) Digital Quantification of Human Eye Color Highlights Genetic Association of Three New Loci. *Plos Genetics* 6.
49. Li Y, Willer CJ, Ding J, Scheet P, Abecasis GR (2010) MaCH: Using Sequence and Genotype Data to Estimate Haplotypes and Unobserved Genotypes. *Genetic Epidemiology* 34: 816–834. <https://doi.org/10.1002/gepi.20533> PMID: 21058334
50. Price AL, Patterson NJ, Plenge RM, Weinblatt ME, Shadick NA, et al. (2006) Principal components analysis corrects for stratification in genome-wide association studies. *Nat Genet* 38: 904–909. <https://doi.org/10.1038/ng1847> PMID: 16862161

51. Pruim RJ, Welch RP, Sanna S, Teslovich TM, Chines PS, et al. (2010) LocusZoom: regional visualization of genome-wide association scan results. *Bioinformatics* 26: 2336–2337. <https://doi.org/10.1093/bioinformatics/btq419> PMID: 20634204
52. Yang J, Lee SH, Goddard ME, Visscher PM (2011) GCTA: a tool for genome-wide complex trait analysis. *Am J Hum Genet* 88: 76–82. <https://doi.org/10.1016/j.ajhg.2010.11.011> PMID: 21167468
53. Willer CJ, Li Y, Abecasis GR (2010) METAL: fast and efficient meta-analysis of genomewide association scans. *Bioinformatics* 26: 2190–2191. <https://doi.org/10.1093/bioinformatics/btq340> PMID: 20616382
54. Pereira TV, Patsopoulos NA, Salanti G, Ioannidis JPA (2010) Critical interpretation of Cochran's Q test depends on power and prior assumptions about heterogeneity. *Research Synthesis Methods* 1: 149–161. <https://doi.org/10.1002/jrsm.13> PMID: 26061380
55. Han B, Eskin E (2011) Random-Effects Model Aimed at Discovering Associations in Meta-Analysis of Genome-wide Association Studies. *American Journal Of Human Genetics* 88: 586–598. <https://doi.org/10.1016/j.ajhg.2011.04.014> PMID: 21565292
56. van Rooij FJA, Qayyum R, Smith AV, Zhou Y, Trompet S, et al. (2017) Genome-wide Trans-ethnic Meta-analysis Identifies Seven Genetic Loci Influencing Erythrocyte Traits and a Role for RBPM5 in Erythropoiesis. *Am J Hum Genet* 100: 51–63. <https://doi.org/10.1016/j.ajhg.2016.11.016> PMID: 28017375
57. Mahajan A, Rodan AR, Le TH, Gaulton KJ, Haessler J, et al. (2016) Trans-ethnic Fine Mapping Highlights Kidney-Function Genes Linked to Salt Sensitivity. *Am J Hum Genet* 99: 636–646. <https://doi.org/10.1016/j.ajhg.2016.07.012> PMID: 27588450
58. Coordinators NR (2016) Database resources of the National Center for Biotechnology Information. *Nucleic Acids Res* 44: D7–19. <https://doi.org/10.1093/nar/gkv1290> PMID: 26615191
59. Aken BL, Ayling S, Barrell D, Clarke L, Curwen V, et al. (2016) The Ensembl gene annotation system. *Database-the Journal Of Biological Databases And Curation*.
60. Ward LD, Kellis M (2012) HaploReg: a resource for exploring chromatin states, conservation, and regulatory motif alterations within sets of genetically linked variants. *Nucleic Acids Research* 40: D930–D934. <https://doi.org/10.1093/nar/gkr917> PMID: 22064851
61. Zhang YB, Wong CH, Birnbaum RY, Li GL, Favaro R, et al. (2013) Chromatin connectivity maps reveal dynamic promoter-enhancer long-range associations. *Nature* 504: 306–+. <https://doi.org/10.1038/nature12716> PMID: 24213634
62. Davydov EV, Goode DL, Sirota M, Cooper GM, Sidow A, et al. (2010) Identifying a High Fraction of the Human Genome to be under Selective Constraint Using GERP plus. *Plos Computational Biology* 6.
63. Siepel A, Bejerano G, Pedersen JS, Hinrichs AS, Hou MM, et al. (2005) Evolutionarily conserved elements in vertebrate, insect, worm, and yeast genomes. *Genome Research* 15: 1034–1050. <https://doi.org/10.1101/gr.3715005> PMID: 16024819
64. Lonsdale J, Thomas J, Salvatore M, Phillips R, Lo E, et al. (2013) The Genotype-Tissue Expression (GTEx) project. *Nature Genetics* 45: 580–585. <https://doi.org/10.1038/ng.2653> PMID: 23715323
65. Lappalainen T, Sammeth M, Friedlander MR, 't Hoen PAC, Monlong J, et al. (2013) Transcriptome and genome sequencing uncovers functional variation in humans. *Nature* 501: 506–511. <https://doi.org/10.1038/nature12531> PMID: 24037378
66. Sanjana NE, Shalem O, Zhang F (2014) Improved vectors and genome-wide libraries for CRISPR screening. *Nat Methods* 11: 783–784. <https://doi.org/10.1038/nmeth.3047> PMID: 25075903
67. Gautier M, Vitalis R (2012) rehh: an R package to detect footprints of selection in genome-wide SNP data from haplotype structure. *Bioinformatics* 28: 1176–1177. <https://doi.org/10.1093/bioinformatics/bts115> PMID: 22402612
68. Voight BF, Kudaravalli S, Wen XQ, Pritchard JK (2006) A map of recent positive selection in the human genome (vol 4, pg 154, 2006). *Plos Biology* 4: 659–659.
69. Findley K, Oh J, Yang J, Conlan S, Deming C, et al. (2013) Topographic diversity of fungal and bacterial communities in human skin. *Nature* 498: 367–370. <https://doi.org/10.1038/nature12171> PMID: 23698366